Direct Single Molecule Imaging of Enhanced Enzyme Diffusion

Mengqi Xu and Jennifer L. Ross
Department of Physics, University of Massachusetts, Amherst, Massachusetts 01003, USA

Lyanne Valdez and Aysuman Sen
Department of Chemistry, Pennsylvania State University, State College, Pennsylvania 18602, USA

(Received 20 November 2018; revised manuscript received 15 March 2019; published 17 September 2019)

Recent experimental results have shown that enzymes can diffuse faster when they are in the presence of their reactants (substrate). This faster diffusion has been termed enhanced diffusion. Fluorescence correlation spectroscopy (FCS), which has been employed as the only method to make these measurements, relies on analyzing the fluctuations in fluorescence intensity to measure the diffusion coefficient of particles. Recently, artifacts in FCS measurements due to its sensitivity to environmental conditions have been evaluated, calling prior enhanced diffusion results into question. It behooves us to adopt complementary and direct methods to measure the mobility of enzymes. Herein, we use a technique of direct single molecule imaging to observe the diffusion of individual enzymes in solution. This technique is less sensitive to intensity fluctuations and deduces the diffusion coefficient directly based on the trajectory of the enzyme. Our measurements recapitulate that enzyme diffusion is enhanced in the presence of its substrate and find that the relative increase in diffusion of a single enzyme is even higher than those previously reported using FCS. We also use this complementary method to test if the total enzyme concentration affects the relative increase in diffusion and if the enzyme oligomerization state changes during its catalytic turnover. We find that the diffusion increase is independent of the total concentration of enzymes and the presence of substrate does not change the oligomerization state of enzymes.

DOI: 10.1103/PhysRevLett.123.128101

Enzymes are reactive nanoscale biomolecules that use energy to perform a variety of tasks required for the basic functions of cells. Enzymes catalyze numerous reactions that are essential to maintain cellular temperature, basic metabolism, and active mixing of the crowded and viscoelastic environment inside cells [1,2]. When enzymes are bound to the surface of nanoscale or microscale colloidal particles, these particles become active and self-propelled in the presence of reactant molecules (substrate) [3–5]. Thus, enzymes have been shown to act as a source of propulsion to move large-scale objects in aqueous media.

Recent experimental studies have demonstrated that enzymes could diffuse faster in the presence of their corresponding enzymatic substrates, which is termed *enhanced diffusion* [6–13]. Prior studies of enhanced diffusion measured a relative increase in the diffusion coefficient from 20% to 80%, depending on the enzyme type used and the substrate concentration [6–13]. A major drawback of prior measurements is that they all used a single method: fluorescence correlation spectroscopy (FCS). In FCS, the diffusion coefficient is determined by measuring and analyzing the autocorrelation function of the fluctuations in fluorescence intensity due to particle motion. Although FCS is referred to as a single molecule technique, the measurement often relies on signals from several particles [14]. Further, it is difficult for FCS to detect if diffusion is anomalously fast (superdiffusive) or slow (subdiffusive), because it typically does not report on the mean squared displacement (MSD) of the particles [15].

A recent publication evaluated possible artifacts of FCS measurements on enzyme diffusion [13]. They demonstrated that enzymes at low concentration can dissociate into smaller subunits, thus causing an increase in diffusion coefficient, but this oligomerization state change cannot be detected by FCS. They also described that free dyes remaining in solution and the binding between enzyme and substrate can affect the measured autocorrelation functions, which subsequently impacted the determination of diffusion rates [13]. Experts agree that interpretation of autocorrelation curves is complicated and requires modeling to fit properly. Yet, prior reports all have fit data with the assumption of normal, free diffusion of enzymes. Thus, it is imperative that these results are verified and recapitulated with distinct experimental methods. Here, we use direct single molecule imaging to visualize the trajectories of diffusing enzymes in solution over time, calculate the mean squared displacements, test if the enhanced diffusion is anomalous, and determine the diffusion coefficients. Our method has the added value that it is truly single molecule and mobility increases are obvious by eye.

Our single particle tracking experiments are performed with total internal reflection fluorescence (TIRF) microscopy

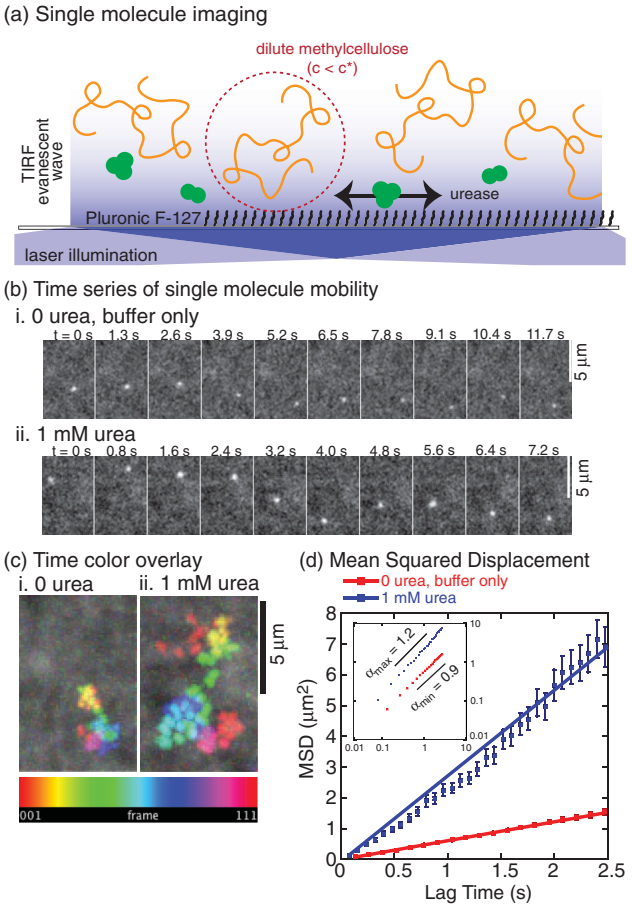

FIG. 1. (a) Experimental setup for single particle imaging of fluorescent urease (green) using TIRF (blue) in a chamber with Pluronic F127 (black) coating the surface and dilute methylcellulose polymers (orange) to slow down the mobility. Radius of gyration of methylcellulose (dashed red circle, ~30 nm) was represented [17]. (b) Example time series of single urease diffusing over time (i) without urea and (ii) with 1 mM urea. Scale bar 5 μm. (c) 2D trajectories displayed as time collapsed images with rainbow scale representing diffusion time over 111 frames with (i) 0.13 s frame interval for urease without urea and (ii) 0.08 s frame interval for urease with 1 mM urea. Scale bar 5 μm. (d) Time-averaged MSD plot of each trajectory before, fitting with a linear equation to determine the diffusion coefficient D. Inset: Same MSD data plotted on log-log scale. Black lines represent the range of α exponent values: $\alpha_{\max} = 1.2$, $\alpha_{\min} = 0.9$. Red squares, urease without urea; blue squares, urease with 1 mM urea; error bars represent the standard error.

[Fig. 1(a)] using a custom-built laser system (488 nm, 638 nm) constructed around a Nikon Ti-E microscope with a 60×, 1.49 numerical aperture TIRF objective and 2.5× magnification prior to the electron multiplier CCD camera (Andor). We directly observe the diffusing trajectory of each individual enzyme by recording at 8–20 frames/s [Figs. 1(b) and 1(c)]. The enzyme used is urease from Jack Bean (TCI Chemicals), a fast, highly exothermic enzyme, that breaks down its substrate, urea, into ammonia and carbon dioxide. Urease is a hexamer which we fluorescently label to a ratio of one fluorophore per monomer, on average, using a commercially available protein labeling kit (Thermo Fisher). Enzymes are blocked from sticking to the silanized hydrophobic cover glass by adding Pluroinc F127 block copolymer to create a polymer brush on the glass surface. The lifetime of the fluorescence is extended by adding glucose oxidase, catalase, and glucose as an oxygen scavenging system, which is exactly the same for all experiments. TIRF microscopy can only image the first 300 nm distance from the cover glass [Fig. 1(a)], so all experiments include the addition of 0.6% 88 kD methylcellulose as a viscous agent to slow down the diffusion. The methylcellulose concentration is in the dilute regime, and polymers are not cross-linked [Fig. 1(a)]. The addition of the methylcellulose slows down the absolute diffusion coefficients we measured by 2 orders of magnitude, but does not affect the relative changes in diffusion measured or trends of the data. Trajectories of enzymes are analyzed by an ImageJ/FIJI plug-in ParticleTracker 2D/3D [16] [Fig. 1(c)], and the time-average MSD is computed for each trajectory: $\langle[\Delta r_i(t)]^2\rangle = \langle[\vec{r}_i(\tau + t) - \vec{r}_i(\tau)]^2\rangle_\tau$.

To test for anomalous diffusion, MSD data are plotted on log-log scale and fit to the power-law equation, $\langle(\Delta r)^2\rangle = \Gamma t^\alpha$, where t is the lag time, Γ is the generalized diffusion coefficient, and α is the anomalous diffusion exponent [Fig. 1(d)]. We find that α was on average equal to one for all data, implying that the diffusion we measure is not anomalous [Fig. 1(d) herein and Fig. S1 of Supplemental Material [18]). Since the MSD is linear with time, we can then deduce the diffusion coefficient D from the slope of the MSD plot according to the normal Brownian motion in 2D: $\langle(\Delta r)^2\rangle = 4Dt$ [Fig. 1(d)].

In agreement with prior work, we find that urease displays enhanced diffusion in the presence of its substrate, urea [Fig. 1(d) and Fig. S1 of Supplemental Material [18]). The change in mobility is visible directly from trajectories and the MSD plots [Figs. 1(b)–1(d)]. For our assays, we measure over 100 single particle trajectories for each experimental condition to obtain statistically significant data. Diffusion data display a log-normal distribution that could be plotted and fit with a Gaussian after log transformation [Fig. 2(a)]. The mean of the Gaussian fit represents the median of the original log-normal distribution, which is then transformed back and used as the effective diffusion coefficient measured for each case (see Supplemental Material for fits and details on the methods [18]).

Interestingly, we find that the relative increase of the diffusion coefficient in our single molecule experiments is significantly higher than those previously reported using FCS methods [7,10]. For the highest concentration of urea we tested (100 mM), we find approximately a threefold increase in the diffusion constant [Fig. 2(b)], compared to prior results that showed only a ~30% increase [7,10].

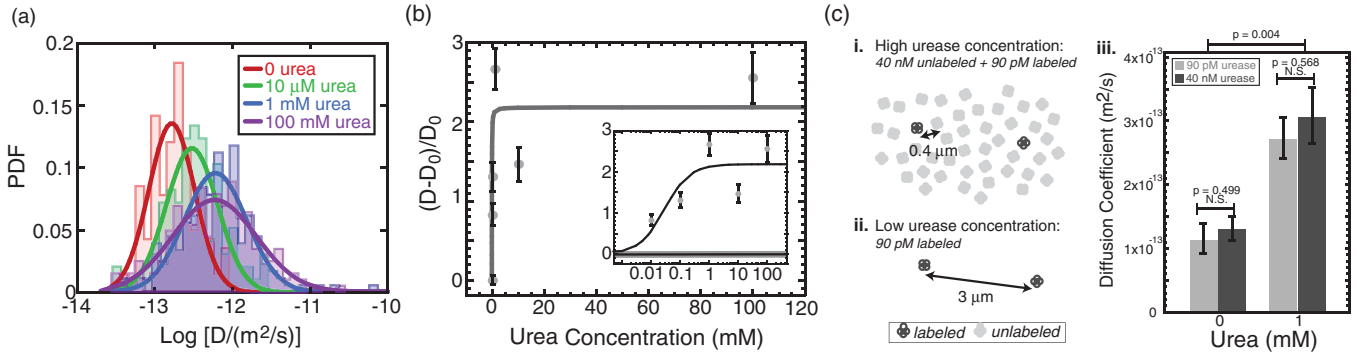

FIG. 2. (a) Representative probability distribution histograms of log-transformed diffusion data at different urea concentrations: 0 (red region, $N = 141$), 10 μM (green region, $N = 97$), 1 mM (blue region, $N = 178$), 100 mM (purple region, $N = 203$), and corresponding Gaussian fit lines 0 (red line), 10 μM (green line), 1 mM (blue line), 100 mM (purple line). (b) The normalized relative increase in the diffusion coefficient $(D - D_0)/D_0$, plotted as a function of the urea concentration. Inset: Same data plotted on a logarithmic scale. Solid line shows the hyperbolic fit with a characteristic concentration K. (c) (i) Illustration of 40 nM urease with average spacing between molecules of 400 nm. (ii) Illustration of 90 pM urease with average spacing between molecules of 3 μm. (iii) Diffusion coefficients of urease at 40 nM urease concentration (dark gray bars) without urea ($N = 31$) and with 1 mM urea ($N = 35$), or urease at 90 pM (light gray bars) without urea ($N = 30$) and with 1 mM urea ($N = 36$). Error bars are determined from the standard errors of the mean of the Gaussian fits. All fit parameters are given in Supplemental Material [18]. PDF: probability distribution function, N.S.: not significant.

Control experiments performed with green fluorescent protein and inhibited urease that cannot interact with urea both show a slight decrease in the diffusion coefficient in the presence of urea (Figs. S2–S4 of Supplemental Material [18]). These controls demonstrate that the enhanced diffusion of urease is not due to the presence of urea in solution, but rather to the interaction between urea and urease.

We calculate and plot the relative increase in the diffusion coefficient as a function of urea concentration [Fig. 2(b)]. The data display a hyperbolic dependence of the form $(D - D_0)/D_0 = A \times ([\text{urea}]/[\text{urea}] + K)$, where D is the measured diffusion coefficient, D_0 is the diffusion coefficient in the absence of substrate, A is an amplitude, [urea] is the urea concentration, and K is the characteristic concentration required for 50% activity. The hyperbolic relationship represents a well-known biochemical model for substrate consumption by enzymes, called the Michaelis-Menten function. We find that the best fit has $K = 30 \pm 30$ μM (all fit parameters available in Supplemental Material [18]).

The equilibrium dissociation constant K_D is the concentration required for half of the maximum urea binding to urease and was previously reported as 250 μM [22]. The Michaelis-Menten constant K_M is the urea concentration required for half the maximum reaction rate of urea consumption by urease and was reported as 3 mM [23]. Comparing our results to these two rate constants, we find that our data are more similar to the binding coefficient K_D instead of the reaction turnover rate K_M. Several theoretical models have suggested that substrate binding could change the size or flexibility of enzymes, driving the difference in the diffusion coefficient [11,24], but no model has predicted such a large shift in the diffusion coefficient as we measured here.

Prior works have noticed a correlation between the diffusion coefficient increase and the heat released during enzymatic turnover [10]. Assuming the enzyme size does not change during the turnover, in order for the diffusion coefficient to increase by a factor of 3, as we observed [Fig. 2(b), the temperature would need to increase by 55 K locally. This increase was estimated by using the Stokes-Einstein relation, $D = k_B T/6\pi\eta R$, in which the viscosity η is also considered as a function of temperature: $\eta(T) = 2.4 \times 10^{-5}\ \text{Pa s} \times 10^{247.8\ \text{K}/(T-140\ \text{K})}$ for water [25]. Using estimation methods described previously [10,26], the temperature increase around a single enzyme ranges from $\Delta T \sim 10^{-11}$ to 0.09 K for urease. All of these estimates, described in detail in the Supplemental Material [18], are too small to account for the factor of 3 increase in diffusion that we observed.

In prior estimations of temperature changes, the enzymes each act as independent sources of heat or activity. Two recent models have taken collective effects of many enzymes into account. One is a collective heating model [26] and the other is a collective hydrodynamics model [27]. Both of these models predict that the diffusion rate increase will depend linearly on the total concentration of the enzymes in solution.

To test the predictions of these collective models, we repeat our experiments at two different total enzyme concentrations, 40 nM and 90 pM [Fig. 2(c)]. For both groups, we keep the concentration of labeled enzyme constant at the single molecule level (90 pM). The average spacing between enzymes depends on their concentration in solution, which we estimate as ~400 nm for 40 nM and ~3 μm for 90 pM [Figs. 2(c)(i) and (c)(ii)]. We compare the diffusion coefficients for different concentration groups in the absence of urea or with 1 mM urea (saturating

concentration, Fig. 2(b)]. We find no difference in the diffusion constants between 40 nM and 90 pM concentrations for either the buffer case or the urea case [Fig. 2(c)(iii)]. Although the proportional relationship between diffusion and total enzyme concentration is not observed in our experiments, it is possible that collective phenomena would come into play at much higher, nonphysiological concentrations of enzymes. Regardless, these collective models cannot explain the threefold increase in diffusion that we observe in our experiments.

Diffusion coefficients can also be significantly altered due to the dissociation of enzyme complexes at the low concentrations used in FCS or single molecule studies, as described above [13].

Suppose an enzyme with radius R undergoes a change in size δR during its interaction with the substrate, the liquid viscosity remains the same. From the Stokes-Einstein equation, the relative change in diffusion can be written as

$$\frac{\Delta D}{D_0} = \frac{1}{1+\frac{\delta R}{R}}\frac{T}{T_0} - 1. \tag{1}$$

A positive change in ΔD requires a negative change in δR, as expected. We can then estimate the size change of urease in our experiments needed to account for a threefold increase in diffusion. For our experiments, $\Delta D/D_0 \sim 2$ and $T/T_0 \simeq 1$ from the calculations above. We estimate that $\delta R \simeq -(2/3)R$, a 67% loss of radius. Considering that urease enzymes are hexamers [28], the large increase in our diffusion measurements would most likely be due to the dissociation of hexamers to smaller oligomers after interacting with urea.

Although this dissociation process cannot be detected by FCS, it can be directly monitored using our single molecule imaging method. To directly test the oligomerization state of the urease multimers, we perform single molecule photobleaching experiments that reveal the number of urease monomers within each fluorescent complex [29,30]. Each urease monomer is covalently labeled with one fluorophore, on average, and there are reported to be 6 monomers per urease complex [28]. We first mix the labeled urease hexamers with urea at 0 or 1 mM concentration, allowing them to react and then affix them to the cover glass. Binding to the glass stabilizes their state and makes the local laser illumination and z height constant for the entire measurement. We use TIRF microscopy to image the enzymes without oxygen scavenging agents, so that the fluorophores photobleach over time [Fig. 3(a)].

We count the number of photobleaching steps for each fluorescent spot, which corresponds to the number of monomers in each complex, and create a histogram of the number of bleaching events for each condition [Fig. 3(b)]. Urease complexes never display more than 6 bleach steps, indicating that the hexamer is the largest oligomerization state. We find that two or three monomers per complex are

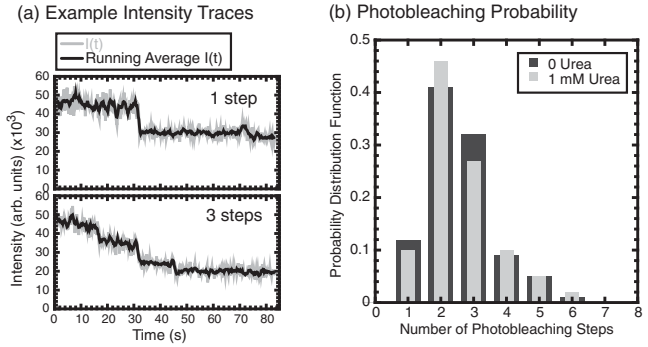

FIG. 3. (a) Two example intensity traces of fluorescent urease complexes photobleaching over time, showing a one-step bleach (top) and a three-step bleach (bottom). (b) The distributions of photobleaching steps directly report the number of fluorescent urease monomers in each complex in the presence of 0 urea (dark gray bars, $N = 100$) and 1 mM urea (light gray bars, $N = 100$).

the most common states for both 0 and 1 mM urea conditions. If the dissociation of the oligomer occurs due to the presence of urea, we would expect to see a large shift in the distribution of the 1 mM urea group to lower numbers of bleaching steps. However, we find no difference between these two distributions according to the Kolmogorov-Smirnov statistical test ($P = 1.0$). From these results, the enhanced diffusion we observe cannot be caused by changes in the oligomerization state of the molecule.

There is a distinct possibility that our technique cannot probe, which is that the shape of the enzyme complex could significantly change from triangular, as depicted in crystal structures [28], to linear (Fig. S5 of Supplemental Material [18]). Because asymmetric particles are known to diffuse faster in the direction parallel to their long axis [31,32], shape changes like these could result in enhanced diffusion by as much as a factor of 2 for urease. Such large shifts in conformation could be probed in future experiments using Förster resonance energy transfer measurements coupled with FCS or single molecule imaging.

In conclusion, we use a distinct method to measure the diffusion of enzymes to test if the enhanced diffusion previously reported was genuine or an artifact of the FCS technique employed. Excitingly, we have verified that the enhanced diffusion of urease occurs on a truly single molecule level. We find that the enhanced diffusion is Brownian—not anomalous. We also observe a higher increase in diffusion rates, by a factor of 3, in comparison with the ~30% increase previously reported. The large increase in diffusion is difficult to account for based on current physical models of heat release or collective interactions. Finally, single molecule imaging techniques are able to directly measure the oligomerization state of the enzymes, excluding the possibility that the enhancement in diffusion we observe is caused by the dissociation of enzyme multimers. We expect that the direct imaging

technique will be a powerful, complementary method to test the predictions of future models of the mechanism behind the enhanced diffusion of enzymes.

M. X. was partially supported by NSF MRSEC DMR-1420382 to Seth Fraden (Brandeis University) and Faculty Research Grant to J. L. R. J. L. R. was partially supported by DoD ARO MURI 67455-CH-MUR to S. Thayumanavan. We want to thank Ramin Golestanian for helpful feedback about our manuscript.

[1] M. Guo, A. J. Ehrlicher, M. H. Jensen, M. Renz, J. R. Moore, R. D. Goldman, J. Lippincott-Schwartz, F. C. Mackintosh, and D. A. Weitz, Cell **158**, 822 (2014).
[2] B. R. Parry, I. V. Surovtsev, M. T. Cabeen, C. S. O'Hern, E. R. Dufresne, and C. Jacobs-Wagner, Cell **156**, 183 (2014).
[3] X. Ma, A. Jannasch, U. R. Albrecht, K. Hahn, A. Miguel-López, E. Schäffer, and S. Sánchez, Nano Lett. **15**, 7043 (2015).
[4] T. Patiño, N. Feiner-Gracia, X. Arqué, A. Miguel-López, A. Jannasch, T. Stumpp, E. Schäffer, L. Albertazzi, and S. Sánchez, J. Am. Chem. Soc. **140**, 7896 (2018).
[5] K. K. Dey, X. Zhao, B. M. Tansi, W. J. Mendez-Ortiz, U. M. Cordova-Figueroa, R. Golestanian, and A. Sen, Nano Lett. **15**, 8311 (2015).
[6] H. Yu, K. Jo, K. L. Kounovsky, J. J. D. Pablo, and D. C. Schwartz, J. Am. Chem. Soc. **131**, 5722 (2009).
[7] H. S. Muddana, S. Sengupta, T. E. Mallouk, A. Sen, and P. J. Butler, J. Am. Chem. Soc. **132**, 2110 (2010).
[8] S. Sengupta, K. K. Dey, H. S. Muddana, T. Tabouillot, M. E. Ibele, P. J. Butler, and A. Sen, J. Am. Chem. Soc. **135**, 1406 (2013).
[9] S. Sengupta, M. M. Spiering, K. K. Dey, W. Duan, D. Patra, P. J. Butler, R. D. Astumian, S. J. Benkovic, and A. Sen, ACS Nano **8**, 2410 (2014).
[10] C. Riedel, R. Gabizon, C. A. M. Wilson, K. Hamadani, K. Tsekouras, S. Marqusee, S. Presse, and C. Bustamante, Nature (London) **517**, 227 (2015).
[11] P. Illien, X. Zhao, K. K. Dey, P. J. Butler, A. Sen, and R. Golestanian, Nano Lett. **17**, 4415 (2017).
[12] A. Y. Jee, S. Dutta, Y. K. Cho, T. Tlusty, and S. Granick, Proc. Natl. Acad. Sci. U.S.A. **115**, 14 (2018).
[13] J. P. Günther, M. Börsch, and P. Fischer, Acc. Chem. Res. **51**, 1911 (2018).
[14] K. Bacia, E. Haustein, and P. Schwille, Cold Spring Harbor Protoc. **2014**, 709 (2014).
[15] J. Kubecka, F. Uhlik, and P. Kosovan, Soft Matter **12**, 3760 (2016).
[16] I. F. Sbalzarini and P. Koumoutsakos, J. Struct. Biol. **151**, 182 (2005).
[17] J. W. McAllister, P. W. Schmidt, K. D. Dorfman, T. P. Lodge, and F. S. Bates, Macromolecules **48**, 7205 (2015).
[18] See Supplemental Material at http://link.aps.org/supplemental/10.1103/PhysRevLett.123.128101 for detailed materials and methods, calculations, and supplemental figures with control experimental data, which includes Refs. [19–21].
[19] N. Tarantino, J. Y. Tinevez, E. F. Crowell, B. Boisson, R. Henriques, M. Mhlanga, F. Agou, A. Israël, and E. Laplantine, J. Cell Biol. **204**, 231 (2014).
[20] J. R. Howse, R. A. L. Jones, A. J. Ryan, T. Gough, R. Vafabakhsh, and R. Golestanian, Phys. Rev. Lett. **99**, 048102 (2007).
[21] J. Cazes, *Encyclopedia of Chromatography* (CRC Press, Boca Raton, FL, 2001).
[22] B. R. J. Tanis and A. W. Naylor, Biochem. J. **108**, 771 (1968).
[23] B. Krajewska, J. Mol. Catal. B Enzym. **59**, 9 (2009).
[24] P. Illien, T. Adeleke-Larodo, and R. Golestanian, Europhys. Lett. **119**, 40002 (2017).
[25] T. Al-Shemmeri, *Engineering Fluid Mechanics* (Bookboon, 2012).
[26] R. Golestanian, Phys. Rev. Lett. **115**, 108102 (2015).
[27] A. S. Mikhailov and R. Kapral, Proc. Natl. Acad. Sci. U.S.A. **112**, E3639 (2015).
[28] A. Balasubramanian and K. Ponnuraj, J. Mol. Biol. **400**, 274 (2010).
[29] J. L. Ross, K. Wallace, H. Shuman, Y. E. Goldman, and E. L. Holzbaur, Nat. Cell Biol. **8**, 562 (2006).
[30] L. Conway, D. Wood, E. Tuzel, and J. L. Ross, Proc. Natl. Acad. Sci. U.S.A. **109**, 20814 (2012).
[31] Y. Han, A. M. Alsayed, M. Nobili, J. Zhang, T. C. Lubensky, and A. G. Yodh, Science **314**, 626 (2006).
[32] C. Ribrault, A. Triller, and K. Sekimoto, Phys. Rev. E **75**, 021112 (2007).